Behavioral/Systems/Cognitive

Transient Extracellular Glutamate Events in the Basolateral Amygdala Track Reward-Seeking Actions

Kate M. Wassum,[1,2,3] Vanessa M. Tolosa,[5] Tina C. Tseng,[6] Bernard W. Balleine,[7] Harold G. Monbouquette,[4] and Nigel T. Maidment[2,3]

[1]Department of Psychology, [2]Department of Psychiatry and Biobehavioral Sciences, Semel Institute for Neuroscience and Human Behavior, [3]Brain Research Institute, and [4]Department of Chemical Engineering, University of California, Los Angeles, Los Angeles, California 90095, [5]Lawrence Livermore National Laboratory, Livermore, California 94550, [6]Department of Chemical Engineering, National Taiwan University of Science and Technology, Taipei 106, Taiwan, and [7]Brain and Mind Research Institute, University of Sydney, New South Wales 2006, Australia

The ability to make rapid, informed decisions about whether or not to engage in a sequence of actions to earn reward is essential for survival. Modeling in rodents has demonstrated a critical role for the basolateral amygdala (BLA) in such reward-seeking actions, but the precise neurochemical underpinnings are not well understood. Taking advantage of recent advancements in biosensor technologies, we made spatially discrete near-real-time extracellular recordings of the major excitatory transmitter, glutamate, in the BLA of rats performing a self-paced lever-pressing sequence task for sucrose reward. This allowed us to detect rapid transient fluctuations in extracellular BLA glutamate time-locked to action performance. These glutamate transients tended to precede lever-pressing actions and were markedly increased in frequency when rats were engaged in such reward-seeking actions. Based on muscimol and tetrodotoxin microinfusions, these glutamate transients appeared to originate from the terminals of neurons with cell bodies in the orbital frontal cortex. Importantly, glutamate transient amplitude and frequency fluctuated with the value of the earned reward and positively predicted lever-pressing rate. Such novel rapid glutamate recordings during instrumental performance identify a role for glutamatergic signaling within the BLA in instrumental reward-seeking actions.

Introduction

The ability to make rapid, informed decisions about whether or not to seek out a reward, such as a palatable food, is essential for survival. Indeed, aberrant reward-related decision making is a hallmark of addiction, obesity, and many other neuropsychiatric disorders. It is therefore imperative to elucidate the neural signals of decision making to understand on a basic level the mechanisms of desire and on a disease level how these signals may be altered to produce maladaptive reward-seeking behavior.

Considerable research efforts, primarily using pharmacological and genetic techniques, have revealed a complex circuitry underlying instrumental reward seeking that includes the amygdala, thalamus, and various cortical regions implicated in decision making (Balleine and Dickinson, 2000; Balleine et al., 2003; Corbit et al., 2003). Within this circuitry, the basolateral amygdala (BLA) appears to be critical for encoding reward value and for use of this information to guide goal-directed actions (Balleine et al., 2003; Wassum et al., 2009a). This region receives excitatory glutamatergic inputs from several areas, but particularly strong direct and indirect reciprocal connections exist with the orbitofrontal cortex (OFC) (Ray and Price, 1992; Carmichael and Price, 1995; Ghashghaei and Barbas, 2002). Indeed, an interaction between the BLA and OFC has been suggested to be necessary for the performance of reward-seeking actions (Pickens et al., 2003; Schoenbaum et al., 2003; Holland and Gallagher, 2004). More generally, activation of ionotropic glutamate receptors is necessary not only for instrumental learning (Kelley, 2004) but also for making informed decisions about whether to seek out reward (Johnson et al., 2005, 2007). What remains to be elucidated is the profile of glutamatergic activity during instrumental behavior, and specifically during the decision-making processes that guide self-initiated action sequences.

This will require direct on-line examination of glutamatergic transmission during the decision-making process, which has been precluded until now by the lack of a method permitting selective measurement of extracellular glutamate with sufficiently high temporal and spatial resolution in freely behaving animals. Here, we take advantage of recent advances in glutamate biosensor technology, developed in our laboratory (Hamdi et al., 2006; Wassum et al., 2008) and elsewhere (Hu et al., 1994; Ryan et al., 1997; Rutherford et al., 2007), to make spatially discrete near-real-time recordings of extracellular glutamate in the BLA during performance of a multiaction, self-paced sequence task for sucrose reward. We identified rapid, transient glutamate

Received Nov. 18, 2011; revised Dec. 22, 2011; accepted Dec. 30, 2011.

Author contributions: K.M.W., B.W.B., H.G.M., and N.T.M. designed research; K.M.W., V.M.T., and T.C.T. performed research; K.M.W. analyzed data; K.M.W. and N.T.M. wrote the paper.

This work was supported by NIDA Grants DA09359 and DA05010, and NINDS Grant NS38367 (N.T.M.); NINDS Grant NS064547 (H.G.M.); an Australian Research Council Laureate Fellowship (B.W.B.); and NIDA Grant DA023774, Hatos Scholarship, and University of California Biotechnology Research and Education Program Graduate Research and Education in Adaptive Biotechnology Fellowship (K.M.W.). We thank Dr. Sean Ostlund for his helpful comments during manuscript preparation.

Correspondence should be addressed to Kate M. Wassum, Department of Psychology, University of California, Los Angeles, 8548 Franz Hall, Los Angeles, CA 90095. E-mail: kwassum@ucla.edu.

DOI:10.1523/JNEUROSCI.5780-11.2012

 0270-6474/12/322734-13$15.00/0

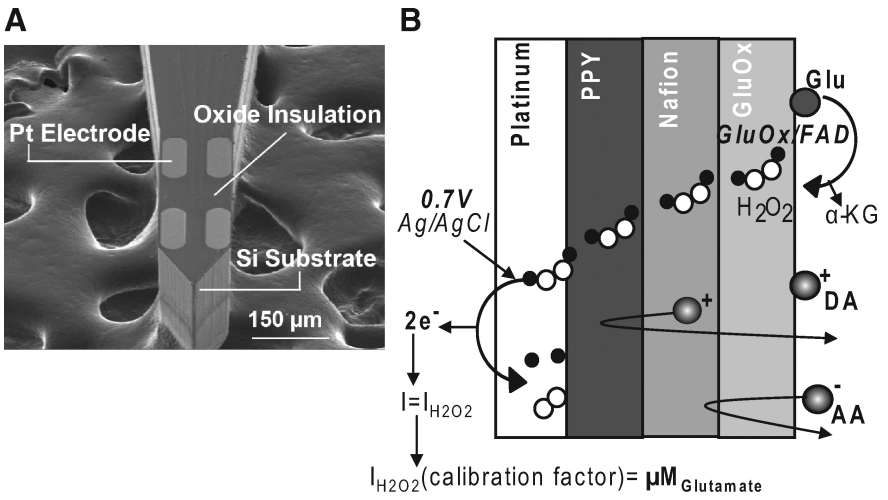

Figure 1. Micromachined silicon-based platinum microelectrode array biosensors for near-real time glutamate detection. ***A***, Scanning electron micrograph image of the tip of the silicon-based probe showing the platinum (Pt) electrode array. The probes were insulated with silicon oxide. ***B***, Schematic representation of the coatings for glutamate biosensing. GluOx is a flavoenzyme that catalyzes the oxidative deamination of glutamate through its flavin adenine dinucleotide (FAD) cofactor, a by-product of which is hydrogen peroxide (H_2O_2). Electrooxidation (at a potential of −0.7 V vs an Ag/AgCl reference electrode) of the enzymatically generated H_2O_2 at the surface of the platinum electrode provides a recordable current signal that, through an *in vitro* calibration factor, can be converted into glutamate concentration. Anions, such as ascorbic acid (AA), are excluded by application of a thin layer of Nafion, while cations, such as dopamine (DA), are repelled from the platinum electrode surface by an electrochemically deposited layer of polypyrrole (PPY).

events, potentially reflective of synaptic overspill, that were time-locked to lever-pressing actions and varied according to task engagement. Such measurements of glutamate transients during free-operant performance provide evidence in support of a role for rapid BLA glutamatergic signaling in the seeking actions that are instrumental to obtaining reward.

Materials and Methods

Glutamate biosensors

Building on previous work (Lowry et al., 1998; Kulagina et al., 1999; Pomerleau et al., 2003; Hamdi et al., 2006), we developed a silicon microprobe-based platinum microelectrode array glutamate biosensor for sensitive, selective, and spatially precise second-to-second measurement of glutamate concentration changes in the brains of freely behaving rats (Fig. 1) (Wassum et al., 2008). These sensors use glutamate oxidase as the biological recognition element for glutamate and rely on electrooxidation (via constant potential amperometry) of enzymatically generated hydrogen peroxide, the current output from which is recorded and converted into glutamate concentration via an *in vitro* calibration factor. Interference from both electroactive anions and cations is effectively excluded from the amperometric recordings, while still maintaining a <1 s response time, by application of Nafion and polypyrrole films to the electrode sites before enzyme immobilization (Wassum et al., 2008). Such selectivity of glutamate detection is a key factor in the sensor design given the presence of dopamine and other electroactive neurotransmitter-containing terminals in the BLA. Furthermore, incorporation of a non-enzyme-coated sentinel electrode on the microelectrode array, signals from which were subtracted from those of the enzyme-coated electrode, provided the noise reduction necessary to reveal rapid transient glutamate events.

Electrode fabrication

The microelectrode array (MEA) probes were fabricated in the Nanoelectronics Research Facility at University of California, Los Angeles. These general procedures have been described previously (Wassum et al., 2008). A 1-µm-thick layer of silicon dioxide was grown thermally on a thin (150–200 µm) silicon substrate. The thermal oxide is a high-quality dielectric film that electrically isolates the substrate from the metal layer subsequently deposited. Electron beam evaporation was used to deposit 1000 Å of platinum on a 200 Å chromium adhesion layer. The metal was patterned by photolithography and lift-off to define the bonding pads, connections, and electrode sites. Next, plasma-enhanced chemical vapor deposition was used to deposit a 1 µm layer of silicon dioxide (5000 Å) and silicon nitride (5000 Å). This second dielectric layer chemically isolates the connections between bonding pads and electrodes. After patterning of the oxide layer with a conventional photolithographic technique, the bonding pads and electrode sites were exposed by reactive ion etching. A third photolithographic treatment was performed to pattern the outline of the probes. Reactive ion etching was then used to etch through the first and second dielectric layers, and deep reactive ion etching by the Bosch process was used to etch through the silicon substrate. The output of the micromachining process was a 4-inch-diameter silicon wafer patterned with 150 MEA probes. The probes were 150 µm thick × 120 µm wide with four platinum electrode sites at the tip. The electrode sites measured ~40 × 100 µm, with a 4800 μm^2 surface area. Horizontally paired electrodes were 40 µm apart, while vertically paired electrodes were 100 µm apart (see Fig. 1*A* for probe tip image). Two electrodes per MEA were used for the experiments here.

After the MEA probes were released individually from the wafer, they were packaged and chemically cleaned to prepare the electrode surfaces for chemical modification with polymers and enzyme. Packaging involved soldering 30 gauge wire to the platinum bonding pads at the top of the MEA. Each MEA was chemically cleaned with isopropyl alcohol and then electrochemically cleaned in 0.5 M H_2SO_4 by cyclic voltammetry from −0.25 to 1.65 V with a scan rate at 50 mV/s for 3 cycles. Following cleaning, the electrodes were dried with argon.

Polymer modification for glutamate detection

The coating schema of an electrode prepared for glutamate detection is represented in Figure 1*B*. Each electrode was coated with polypyrrole (PPy) to repel interference from cations, such as dopamine, and Nafion to electostatically repel anionic interference from molecules such as ascorbic acid and DOPAC (3,4-dihydroxyphenylacetic acid). After the polymer treatments, the enzyme L-glutamate oxidase (GluOx) was immobilized onto select electrode sites to provide the biological recognition element for glutamate detection. The details of electrode modification have been reported previously (Wassum et al., 2008) and are briefly described below. Electrodes coated with PPy/Nafion and GluOx are referred to as glutamate biosensors. All electrodes were calibrated (see below) before implantation.

PPy was electrodeposited by holding the voltage constant at 0.85 V for 2.5–5 min until a total charge density of 20 mC/cm^2 was reached in a 200 mM argon-purged solution of pyrrole in PBS at pH 7.4. The polymer Nafion was deposited on the sites by rapid dip-coating of the probe tips in the Nafion solution and oven casting at 180°C for 3 min, followed by 1 min cooling in ambient air. This process was repeated twice. After the polymer treatments, enzyme immobilization was accomplished by chemical cross-linking using a solution consisting of GluOx (400 U/ml), BSA (6 mg/ml), and glutaraldehyde (0.075%). A ~1 µl drop of the solution was formed on a syringe tip and fixed in place under a microscope. The probe was attached to a micromanipulator (Sutter Instrument) and positioned vertically relative to the enzyme solution droplet. With the aid of the microscope, the MEA was lowered into the enzyme droplet to coat only the bottom two electrodes. This was repeated four to five times with each application consisting of two to three dips. Three days after enzyme immobilization, the PPy was overoxidized by holding the potential applied to the electrode at −0.7 V for 30–45 min in PBS until a stable

baseline was attained during the calibration. The MEAs were then sealed in a container with desiccant and stored at 4°C.

Reagents

Nafion (5 wt % solution in lower aliphatic alcohols/H_2O mix), bovine serum albumin (BSA) (min 96%), glutaraldehyde (25% in water), pyrrole (98%), L-glutamic acid, L-ascorbic acid, and 3-hydroxytyramine (dopamine) were purchased from Sigma-Aldrich. GluOx from *Streptomyces* sp. X119-6, with a rated activity of 24.9 U mg^{-1} (Lowry's method), produced by Yamasa Corporation, was purchased from Associates of Cape Cod (Seikagaku America). PBS was composed of 50 mM Na_2HPO_4 with 100 mM NaCl, pH 7.4. Ultrapure water generated using a Millipore Milli-Q Water System was used for preparation of all solutions used in this work.

Instrumentation

Electrochemical preparation of the sensors was performed using a Versatile Multichannel Potentiostat (model VMP3) equipped with the "p" low current option and low current *N′* stat box (Bio-Logic). *In vitro* and *in vivo* measurements were conducted using a multichannel Fast-16 potentiostat (Quanteon), with reference electrodes consisting of a glass-enclosed Ag/AgCl wire in 3 M NaCl solution (Bioanalytical Systems) or a 200-μm-diameter Ag/AgCl wire, respectively. All potentials are reported versus the Ag/AgCl reference electrode.

In vitro *electrode characterization and data analysis*

Biosensors prepared for glutamate detection were calibrated *in vitro* to test for sensitivity and selectivity to glutamate. A constant potential of 0.7 V was applied to the working electrodes against an Ag/AgCl reference electrode in 40 ml of stirred PBS at pH 7.4 and 37°C within a Faraday cage. Data were collected at 80 kHz and averaged over 1 s intervals. After the current detected at the electrodes equilibrated to baseline (~30–45 min), aliquots of glutamate were added to the beaker to reach final glutamate concentrations in the range 5–60 μM. A calibration factor based on analysis of these data was calculated for each electrode on the MEAs to be used for *in vivo* experiments. The average calibration factor for the sensors used in these experiments was 149.6 μM/nA. Additionally, aliquots of ascorbic acid (250 μM final concentration) and dopamine (5–10 μM final concentration) were added to the beaker as representative examples of readily oxidizable potential anionic and cationic interferent neurochemicals, respectively, to confirm selectivity for glutamate. No current changes above the level of the noise were detected to the addition of these interferents, as we have reported previously (Wassum et al., 2008). To assess the sensitivity and response time to peroxide at sites uncoated with enzyme, aliquots of H_2O_2 were also added to the beaker. Importantly, electrodes coated with PPy and Nafion only, but not GluOx, showed no detectable response to glutamate, despite being sensitive to H_2O_2. Indeed, there was a $<10\%$ statistically insignificant ($t_{(15)} = 1.68$; $p = 0.11$) difference in the H_2O_2 sensitivity on control electrode sites relative to enzyme-coated sites, indicating that any changes detected *in vivo* on the enzyme coated sites could not be attributed to endogenous H_2O_2.

Sensor modification for chronic implantation

For recording in the awake, freely moving rat, connection wires from the MEA and reference electrodes were soldered to gold-plated sockets (Ginder Scientific) and the silicon wafer-based MEA was attached with epoxy to a 9-pin miniature connector (Ginder Scientific) such that all the sockets were encased in the connector. The entire assembly was sealed with epoxy to ensure full insulation and allowed to cure for 1 h before implantation. In some cases (see below), a guide cannula was also epoxied on top of the sensor to allow for local infusions around the sensor *in vivo*.

Behavioral training

Subjects

Male Sprague Dawley rats ($N = 23$) weighing between 240 and 320 g were group housed and handled daily for 3 d before instrumental training. Training and testing took place during the light phase of the 12 h light/dark cycle. Rats were maintained on a food-deprived schedule whereby they received 10–12 g of their maintenance diet daily to maintain 85% *ad libitum* feeding body weight. All rats were fed ~3 h after the training session of each day, and all food was normally consumed within 1 h. Rats had *ad libitum* access to tap water in the home cage. All procedures were conducted in accordance with the *Guide for the Care and Use of Laboratory Animals* and approved by the University of California, Los Angeles, Institutional Animal Care and Use Committee.

Apparatus

Training and testing took place in a MED Associates operant chamber housed within a sound- and light-resistant shell. The chamber contained two retractable levers that could be inserted to the left and right of the magazine. A 3 W, 24 V house light mounted on the top of the center wall opposite the magazine provided illumination. The chamber was equipped with a pellet dispenser that delivered a single 45 mg sucrose pellet (Bio-Serv) into a small well mounted on the front wall of the chamber.

Behavioral task

Single action-outcome reward-seeking scenarios are rare in reality. Therefore, we trained rats on a self-paced action sequence, a situation that better reflects decision-making problems that humans face in naturalistic settings. The behavioral procedure required rats to perform a fixed sequence of two different lever press actions to earn sucrose pellets, such that one action was temporally distal and the other temporally proximal to reward delivery. The distal lever was continuously available and, when pressed, resulted in the insertion of the proximal lever (a discriminative stimulus) into the chamber. Pressing the proximal lever resulted in the delivery of a sucrose pellet and caused that lever to be retracted. Importantly, this task was self-paced; the rat's decision to engage in the sequence was not precipitated by an experimenter-delivered stimulus; rather, the rat could control both the initiation of each "trial" sequence as well as the speed with which the sequence of actions was performed. In this way, the action sequence required both an initiation action, guided by some form of decision to engage in the sequence, as well as a termination action that directly provided reward delivery. Notably, the use of an action sequence task allowed for two primary behavioral measures to which we could correlate changes in glutamate detected with our glutamate biosensors: lever press rate, a measure of action performance, and action sequence time (the time from the initiating distal lever press through the sequence to the next initiating distal lever press).

Action sequence training

Each session started with the illumination of the house light and insertion of the levers where appropriate and ended with the retraction of the levers and turning off of the house light. Rats received only one training session per day.

Magazine training. Rats received 2 d of magazine training in which they were exposed to noncontingent sucrose pellet deliveries (20 outcomes over 30 min) in the operant chamber with the levers retracted, to learn where to receive the sucrose reinforcement.

Single action instrumental training. Rats were then given 2 d of single-action continuous reinforcement training on the lever to the right of the magazine with the sucrose delivered on a continuous reinforcement schedule. Each session lasted until 20 outcomes had been earned or 30 min elapsed.

Training on the action sequence. On day 5 of instrumental training, the distal lever (i.e., the lever to the left of the magazine) was introduced into the chamber. Initially, only the distal lever was present. One response on the left, distal lever resulted in the presentation of the right, temporally proximal lever, a response on which resulted in delivery of a single sucrose pellet and retraction of the proximal lever. This session continued until 20 outcomes were earned or 30 min elapsed. This training was conducted for five sessions or until stable proximal response rates were attained. At this point, rats underwent surgery for glutamate biosensor implantation.

Monitoring extracellular glutamate concentration changes in the BLA during instrumental action performance

The first experiment was intended to examine the profile of rapid glutamatergic changes in the BLA associated with action sequence performance. After training, rats ($N = 7$) were implanted with a precalibrated glutamate biosensor into the BLA (AP, −3.0 mm; ML, +5.1; DV, −8.0). After a brief recovery period, the biosensor was tethered to the potentiostat (Fast-16; Quanteon) and a potential of 0.7 V was applied, versus a Ag/AgCl reference electrode in the contralateral cortex, for the oxidation of the GluOx-generated H_2O_2 (Wassum et al., 2008). This oxidative current was recorded at 80 kHz and averaged over 0.25 s intervals. Once the recorded amperometric signal equilibrated (~30–45 min), the rat was transferred to the operant chamber and, after a 3 min baseline period, allowed to respond on the action sequence for a total of 30 sucrose pellet rewards. Importantly, rats were not retrained on the action sequence task after sensor implantation before test such that their initial responses (the first five cycles) were considered a "refamiliarization period."

To examine whether changes in the value of the sucrose reward (information that is used to inform decisions) would affect glutamate signaling associated with subsequent action performance, a second set of rats were subjected to a specific satiety reward devaluation procedure. Following biosensor equilibration, rats were transferred to the operant chamber and allowed to respond on the action sequence for a total of 10 sucrose pellet rewards. After this initial refamiliarization period, rats were then transferred back to the holding chamber and were either allowed to consume the sucrose pellets to satiety (for 1 h), or given no satiety treatment (1 h wait period), before being returned to the testing chamber. This sensory-specific satiety procedure is well established to reduce the incentive value of food rewards, reflected by fewer seeking actions for the reward (Berridge, 1991; Dickinson et al., 1996; Balleine et al., 2005; Wassum et al., 2009b). Upon return to the testing chamber, rats were allowed to respond on the sequence of actions again for up to 30 sucrose pellet rewards.

As glutamate can arise from release from both neurons and nonneuronal (i.e., glial) sources, it was imperative to assess the pool from which our glutamate concentration changes arose. Therefore, in a third groups of rats ($N = 4$), we locally infused tetrodotoxin (TTX) into the region surrounding the glutamate biosensor to block action potential-dependent glutamate release. At surgery, this group of rats was implanted with a glutamate biosensor into the BLA as above; however, attached to these sensors was a 7 mm, 22 gauge guide cannula (Plastics One) positioned such that when the 9 mm injector was inserted into the cannula the tip of the injector was ~50–100 μm away from the MEAs. At test, after equilibration, rats were infused with sterile water vehicle (0.3 μl over 1 min). The injector was left in place for an additional minute before being removed. After a 10 min interval, recording commenced while rats were in the recording chamber and lasted for 30 min. After this vehicle session, rats were then infused with TTX (0.3 μl of 100 μM over 1 min; Tocris Bioscience). Again after a 10 min injection test interval, the TTX recording period commenced. Although rats were freely moving, no behavioral tasks were performed during this test based on our preliminary data suggesting that intra-BLA TTX treatment disrupts behavioral performance. The order of testing was not counterbalanced based on our preliminary data suggesting the effects of TTX on glutamate recordings to be long-lasting (i.e., >24 h).

In a fourth group of rats ($N = 4$), we further examined the origin of transient BLA glutamate concentration changes. Glutamatergic inputs to the BLA from the OFC are particularly strong and communication between these structures has been implicated in instrumental action performance. Therefore, we inactivated the ipsilateral OFC while monitoring transient glutamate concentration changes in the BLA of rats performing on the sequence of actions to earn sucrose pellet rewards. For this group, after training on the action sequence, rats were implanted with a precalibrated glutamate biosensor in the BLA along with an ipsilateral 22 gauge guide cannula projected toward the OFC (AP, +3.5 mm; ML, +3.0; DV, −3.4). After a 24 h recovery period, the biosensor was tethered to the potentiostat, a potential of 0.7 V was applied, and the signal was allowed to stabilize (~45 min). Using a microinfusion pump, sterile water vehicle was infused into the OFC in a volume of 0.5 μl over 1 min via an injector inserted into the guide cannula fabricated to protrude 1 mm ventral to the tip. Injectors were left in place for at least 1 additional minute to ensure full infusion. Fifteen minutes thereafter, rats were placed in operant boxes and allowed to respond on the action sequence to earn 10 sucrose pellet rewards. After this session, muscimol (1 μg/μl in sterile water vehicle; Tocris Bioscience) was infused into the OFC at a volume of 0.5 μl over 1 min, with an additional 1 min to ensure infusion. Unilateral infusions were intentionally used here to avoid impacting behavioral performance. Indeed, several reports have shown that lesions of the OFC lead to impulsive choice (Mar et al., 2011) and an inability to update behavior based on a change in reward value (Pickens et al., 2005). Again, 15 min elapsed after muscimol infusion before rats were placed in the operant chamber and allowed to respond on the action sequence for a total of 10 sucrose pellet rewards. The following day, rats were again tethered to the potentiostat and, after signal stabilization, received a second intra-OFC infusion of vehicle 15 min before being placed back in the operant box to respond on the action sequence for a total of 10 sucrose pellet rewards.

Histology

At the conclusion of each experiment, rats were anesthetized with Nembutal and transcardially perfused with 0.9% saline followed by 10% formalin saline. The brains were removed and postfixed in formalin, and then cryosectioned into 60 μm slices, mounted onto slides, and stained with cresyl violet. Light microscopy was used to examine sensor placement in the BLA and where applicable guide cannula placement. Histological data are presented Figure 2.

Data analysis

All data were processed with Microsoft Excel, and then compiled and statistically analyzed, unless otherwise mentioned, with GraphPad Prism and SPSS. In all cases, the threshold for significance was set at $p < 0.05$.

We developed a method of data analysis, derived from the techniques of background-subtracted fast-scan cyclic voltammetry (Michael et al., 1999) and glutamate biosensor self-referencing (Rutherford et al., 2007), wherein the current output from each electrode on the MEA was subtracted from the baseline current for that electrode, determined a 10 s average at the beginning of the 3 min baseline period before the beginning of the lever-pressing test. A representative example of this data output is shown in Figure 3 (the details of this figure are discussed later in Results). We then exploited the utility of the control electrode and subtracted current change from baseline on the PPy/Nafion-coated electrode from the current change from baseline on the PPy/Nafion/GluOx glutamate biosensor to obtain a low-noise change-from-baseline glutamate current signal (see Fig. 3*C*). This technique has the advantage of subtracting all current responses that result from anything other than enzymatically generated H_2O_2 oxidation from the glutamate response, thereby reducing the level of the noise and allowing the small glutamate concentration changes to be revealed. Without such noise reduction analysis, glutamate transients are often barely detectable above the level of the noise.

Mini Analysis (Synaptosoft) was then used on this data output to determine the frequency, amplitude, half-width, and decay time of the transient glutamate events. A fluctuation in the glutamate trace was deemed a glutamate transient if it was at least 2.5 times greater than the root-mean-square noise. To determine the transient amplitude, a baseline was taken as the first minima located 0.5–2 s before the peak. Rise time to peak response was also calculated from this baseline point. Half-width was taken as the width of the peak at one-half of the maximal peak amplitude, and decay time was calculated as the time it took for the current to drop from the peak to 37% of the peak amplitude (see Fig. 4*A*). Representative examples of individual transients taken from four different rats are shown in Figure 4. The majority of transients were ~2–5 s in duration; however, as is seen in Figure 4*D*, on rare occasions some transients lasted longer. A representative glutamate transient frequency and lever press histogram is presented in Figure 3*D*.

After the initial analysis for identification and characterization of BLA glutamate transients, we split the data into three test phases for further

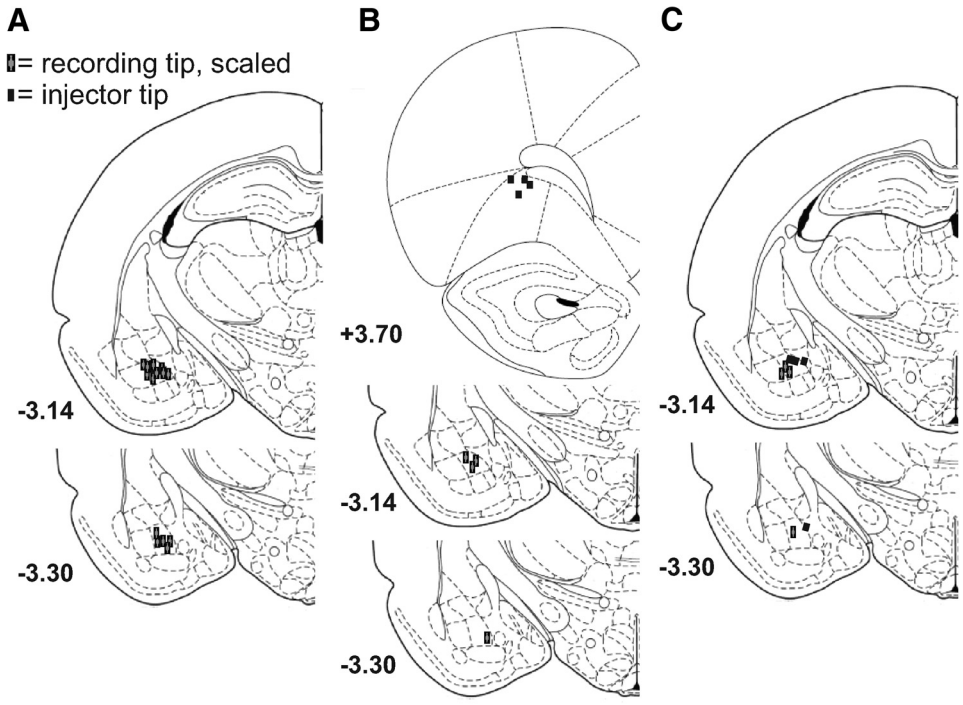

Figure 2. Schematic representation of the placement of MEA biosensor tips and injectors. Line drawings of coronal sections are taken from Paxinos and Watson (1998). Numbers to the bottom right of each section represent the anterior–posterior distance (in millimeters) from bregma of the section. ***A***, The recording tip of the MEA placement for rats in which only the biosensor was implanted in the BLA. Representation is relatively scaled to the coronal line section. ***B***, OFC injector placements along with MEA recording tip placement in the BLA. ***C***, Recording tip of the MEA with attached guide and injector placement for TTX/vehicle infusion in the BLA.

analysis. The 3 min period prior the lever-pressing test session served as the baseline. Since there were long periods of time in which the rats were in the operant chamber and had the opportunity to, but were not engaged in the lever-pressing task, we also divided the behavioral lever-pressing test into two separate phases: task-engaged and unengaged. Task-engaged was defined as the 10 s before or after any lever press event, while unengaged was any time during the lever-pressing test outside this window. These three test phases were used for all subsequent analyses.

Glutamate transient dynamics (amplitude, rise time, half-width, and decay time) were averaged within each phase for each rat, and then averaged across rats. These data were analyzed with a one-way repeated-measure ANOVA with "test phase" as the variable; baseline, in the session but unengaged in the lever-pressing task, or in the session and engaged in lever pressing (i.e., within $\pm$10 s of a lever press event).

Averaged glutamate transient frequency data were analyzed with a one-way repeated-measure ANOVA to examine the effects of test phase on the number of glutamate transients per minute. *Post hoc* analyses were then used to compare glutamate transient frequency during each lever-pressing test phase. After this, a further level analysis was conducted to determine how lever-pressing activity was distributed around transients. We counted all the lever presses in the 10 s before and after every transient and totaled this for each rat, and then averaged this across rats. These data were analyzed for normality (D'Agostino and Pearson Omnibus normality test), skewness, and kurtosis.

As mentioned above, rats were not retrained on the lever-pressing task before test. Given the difference in behavioral output during the refamiliarization (first 5 cycles) and performance periods (last 25 cycles), glutamate transient frequency and amplitude were correlated with lever press rate for only the performance period of the lever-pressing test to avoid the behavioral confound of refamiliarization. Neither glutamate transient frequency ($t_{(6)} = 1.33$; $p = 0.23$) nor amplitude ($t_{(6)} = 0.25$; $p = 0.81$) was significantly different between the refamiliarization and performance phases. The average glutamate transient frequency and amplitude during the performance period of the lever-pressing test (both task-engaged and unengaged phases) for each rat were plotted as a function of press rate, and these data were analyzed with a Pearson correlation.

The average glutamate transient frequency and amplitude for rats that underwent the specific satiety outcome devaluation procedure, together with their unsated controls, were analyzed with a two-way ANOVA with "test phase" as the within-subjects variable and "satiety level" as the between-subjects variable. Bonferroni's *post hoc* analysis was used to compare the effects of satiety in each test phase. Similarly, the average glutamate transient frequency and amplitude for rats receiving infusions of vehicle and muscimol into the OFC were analyzed with a two-way ANOVA with "test phase" and "intra-OFC drug" as the within-subjects variables. Bonferroni's *post hoc* tests were used to compare the effects of drug within each test phase. Glutamate transient frequency following local application of vehicle or TTX was analyzed with a paired *t* test.

The behavioral data for rats receiving the specific satiety treatment were analyzed with a two-way ANOVA to compare the effects of the between-subjects variable "satiety level" on lever press rate, with "lever" as a within-subjects variable (either the distal or proximal response). Similarly, the data from the behavioral session in which rats were pretreated with either intra-OFC vehicle or muscimol were also analyzed with a two-way ANOVA with within-subjects variables, "drug" and "lever."

In addition to this analysis of transient glutamate concentration changes across the entire test session, we also cut the data into 20 s peri-press bins, reflective of the task-engaged phase of the lever-pressing session, to show the averaged transient glutamate concentration surrounding each lever press action. As above, the current output from each electrode on the MEA was subtracted from the baseline current for that electrode. For this analysis, a local baseline was determined as the average of the 2 s before the first distal press in a sequence to specifically look at changes time-locked to lever-pressing activity. The current change from baseline on the control electrode was then subtracted from the current change from baseline on the glutamate biosensor to get a low-noise, interference-free glutamate trace in the 10 s before and after a lever press event. These traces were then averaged across trials for each rat and then across rats; these data are presented in Figure 3, *E* and *F*.

Results

The behavioral procedure required rats to perform a fixed sequence of two different lever press actions to earn sucrose

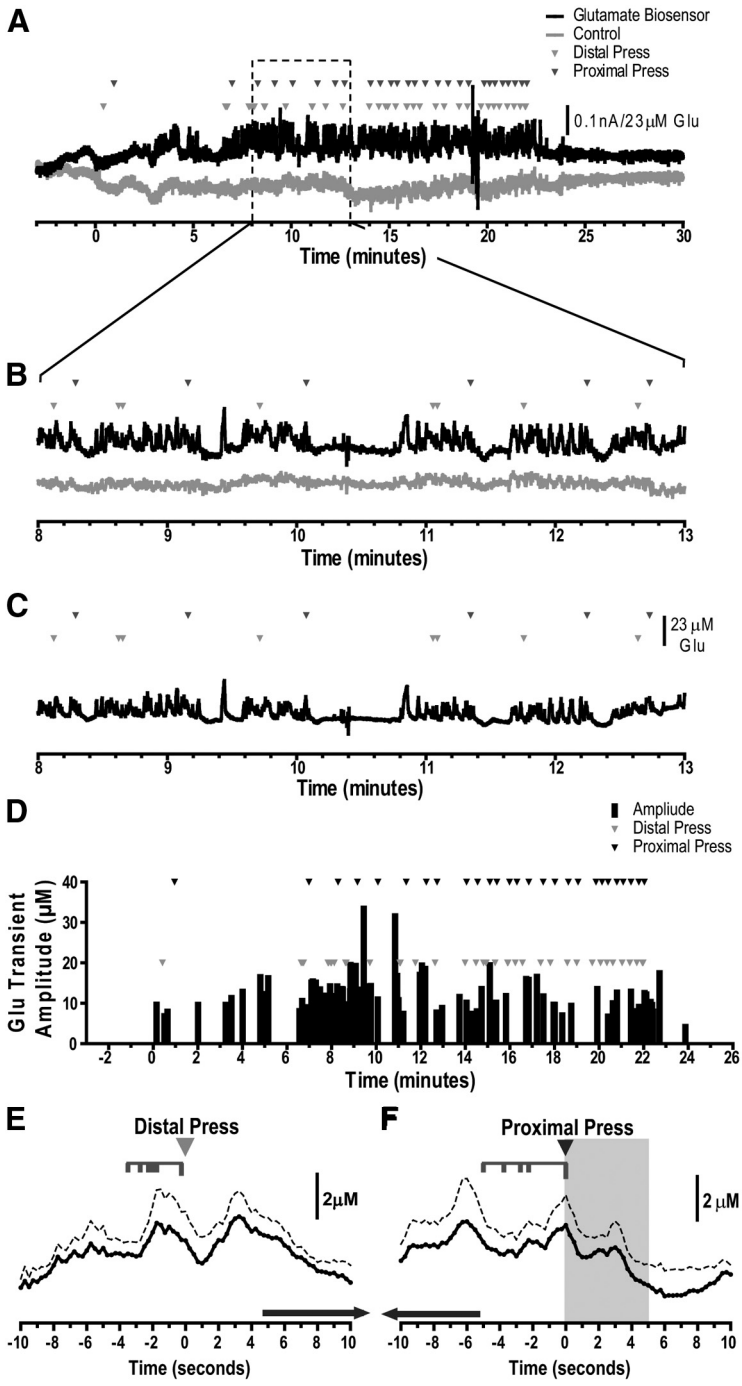

Figure 3. Representative example of transient glutamate concentration changes in the basolateral amygdala. After a 3 min baseline period in the operant chamber, rats were allowed to respond on the sequence of actions to earn sucrose pellet rewards while current changes at both the glutamate biosensor and control electrodes were recorded. The lever-pressing session started at time 0. The light gray triangles reflect distal lever presses, while the dark gray triangles indicate the time of proximal lever presses. ***A***, Current changes recorded from the glutamate biosensor (black line) and control electrode (gray line) were subtracted from the baseline current (average of the 10 s 3 min before the beginning of the lever-pressing test). ***B***, The dashed box of ***A*** is expanded to show a 5 min time frame from the lever-pressing session and clarify the rapid changes detected on the glutamate biosensor output. ***C***, Current changes from baseline on the control electrode were subtracted from current changes from baseline on the glutamate biosensing electrode to provide the extracellular glutamate measurement. ***D***, BLA glutamate transient events (black bars) were counted (see Materials and Methods) over the test session. The time of each event is plotted on the *x*-axis, with transient amplitude plotted on the *y*-axis. ***E***, ***F***, Task-related BLA glutamate concentration changes. Preevent background (average of 10–8 s before distal lever press) subtracted signals from the control electrode were subtracted from the glutamate biosensor signal and time-locked to either the distal (***E***) or proximal (***F***) lever press action. Resulting glutamate concentration changes were averaged within each rat (~30 trials), and then across rats ($N = 7$). The arrows above the *x*-axis indicate the range of the average time (across events within each rat) at which the following proximal (***E***) or preceding distal (***F***) lever press occurred, such that peaks occurring above these arrows reflect glutamate concentration changes associated with the preceding or following event. The gray bar (***E***) marks the 5 s period after the proximal action that coincided with delivery and consumption of the sucrose pellet. The dashed line indicates +1 SEM.

pellets, such that one action was temporally distal and the other temporally proximal to reward delivery. The distal lever was continuously available and, when pressed, resulted in the insertion of the proximal lever into the chamber. Pressing the proximal lever resulted in the delivery of a sucrose pellet and caused that lever to be retracted. Importantly, this task was self-paced; the rat's decision to engage in this action was not precipitated by an experimenter-delivered stimulus; rather, the rat could control both the initiation of each trial sequence as well as the speed with which the sequence of actions was performed. Rats were trained to asymptotic performance (5 d) on this sequence before biosensor implantation and test. All rats acquired and attained stable performance on the sequence of actions. At test, rats performed at an average response rate of 1.85 (SEM, 0.39) presses/min on the distal lever and 1.21 (SEM, 0.129) presses/min on the proximal lever. Since rats were not retrained on the action sequence task after sensor implantation their initial responses may be considered a "refamiliarization phase." In support of this, in the first five pressing cycles, rats displayed a significantly longer latency (20.55 s; SEM, 4.94 s) to press the proximal lever after the distal lever had been pressed (releasing the proximal lever), relative to the remaining 25 "performance phase" pressing cycles (6.05 s; SEM, 0.72 s; $t_{(6)} = 2.97$; $p = 0.02$).

As can be seen in the representative example shown in Figure 3, *A* and *B*, the background-subtracted (see Materials and Methods) baseline glutamate concentration was relatively stable over time during the lever-pressing session (black line, glutamate biosensor output). However, while rats were performing on the sequence of actions to earn sucrose reward, increases in current of relatively short duration were observed coincident with lever-pressing activity (Fig. 3*B*). Such transients were detected in the glutamate biosensor output, but not in the control electrode output (i.e., from the electrode that was not capable of detecting glutamate), and are therefore indicative of rapid glutamate concentration changes. These glutamate transients were further resolved when current changes from baseline on the control electrode were subtracted from current changes from baseline on the glutamate biosensing electrode to reduce the level of the noise (Fig. 3*C*). The representative histogram in Figure 3*D* reveals that transient glutamate concentration change events (elevations in glutamate that were at least 2.5 times greater the root-mean-square

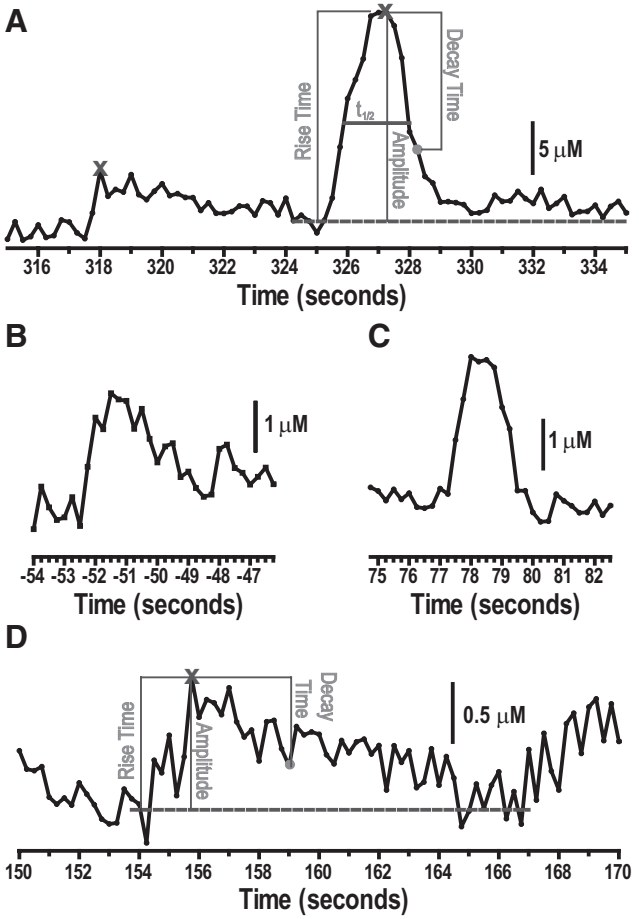

Figure 4. Representative examples of individual basolateral amygdala glutamate concentration transients. Current changes from baseline on the control electrode were subtracted from current changes from baseline on the glutamate biosensing electrode to provide the extracellular glutamate measurement. Time in seconds on the *x*-axis reflects the actual time in the test session from which the transient was extracted, with the lever-pressing test starting at 0 s. ***A***, Representative 20 s time bin from the behavioral session of a single rat showing two glutamate concentration transients. Rise time is calculated as the time from baseline to the peak amplitude of the transient, marked with an "X." The amplitude is calculated as the peak amplitude of the transient minus the baseline. Decay time is calculated as the time from the peak amplitude to 37% of the peak amplitude and $t_{1/2}$ is the width of the peak at one-half of the amplitude. ***B***, ***C***, Representative transients from two separate animals on a shorter 7 s timescale. ***B*** shows a spontaneous transient from the baseline period. ***D***, On some occasions, transients were longer in duration as is shown in this representative transient.

noise) occurred both spontaneously and time-locked to lever-pressing activity (see group analyses below).

Basolateral amygdala glutamate transient dynamics

Representative examples of individual transients taken from four different rats are shown in Figure 4. The vast majority of transients were ~2–5 s in duration (baseline-to-baseline) with rare examples of longer duration (Fig. 4*D*). As can be seen in Table 1, the average rise time of glutamate transients was 0.9 s (SEM, 0.1), with a decay time of 0.6 s (0.008) and a half-width of 0.8 s (0.04). These transient characteristics did not differ with the test phase; there was no significant main effect of test phase on glutamate transient rise time ($F_{(2,20)} = 0.15$; $p = 0.86$), decay time ($F_{(2,20)} = 1.73$; $p = 0.22$), or half-width ($F_{(2,20)} = 1.23$; $p = 0.33$). It is important to note that the temporal properties of these glutamate transients match closely the response time of the sensors in a flow cell (rise time, ~0.8 s) (Wassum et al., 2008). It is likely, therefore, that extracellular glutamate concentration is, in fact, changing more rapidly than these measurements suggest.

Table 1. BLA glutamate transient temporal dynamics

	Transient feature		
Test phase	Rise time (s)	Half-width (s)	Decay time (s)
Baseline			
Mean	0.9	0.9	1
SEM	(0.1)	(0.1)	(0.1)
In session (unengaged)			
Mean	0.8	7	0.8
SEM	(0.1)	(0.04)	(0.1)
Task engaged			
Mean	0.7	0.6	0.6
SEM	(0.03)	(0.02)	(0.02)

BLA glutamate transient temporal dynamics were averaged for each rat across each test session phase and then across rats. Test phases were divided into the 3 min baseline period when the rat was in the operant box prior to the lever-pressing session (baseline), when the rat had the opportunity to, but was not lever pressing (in session, unengaged), and the 10 s prior to and 10 s after any lever press event (task engaged). The mean and SEM are shown. $N = 7$.

The frequency of basolateral amygdala glutamate transients increases during instrumental performance and predicts lever press rate

Examination of glutamate transient frequency across rats shows that glutamate transients occurred more when rats were engaged in the action sequence lever-pressing task. Analysis of transient frequency with respect to test session phase (presession baseline, in pressing session–unengaged, in pressing session–task-engaged/within 10 s of a lever press) revealed a main effect of test phase ($F_{(2,20)} = 16.12$; $p = 0.0004$). *Post hoc* analysis indicated that glutamate transient frequency was significantly elevated from baseline when rats were engaged in the task ($p < 0.001$), but that during the lever-pressing session when rats were not engaged in lever pressing there was no significant change in glutamate transient frequency ($p > 0.05$; Fig. 5*A*). Indeed, within the lever-pressing session the frequency of task-related glutamate transients was significantly higher than those falling outside the peri-press window ($p < 0.01$; Fig. 5*A*). Interestingly, the distribution of presses around glutamate transient events deviated significantly from normality ($K^2 = 7.59$; $p = 0.03$), with a positive skewness (1.29) and kurtosis (1.20), indicating that glutamate transients tended to closely precede lever-pressing activity (Fig. 5*B*). However, it should be noted that 42% (SEM, 11%) of proximal presses were followed immediately (within 5 s) by a glutamate transient, suggesting that these transients also occurred at the conclusion of the sequence when the sucrose pellet reward was consumed. (The tendency for transients to be diminished in frequency during the consumption phase in the example shown in Fig. 3 was not typical.)

These data are supported by analysis of the average glutamate concentration change in the task-engaged window (Fig. 3*E*,*F*). As can see be seen from this figure, there is a clear transient increase in glutamate concentration from baseline preceding both the distal and proximal lever presses (Fig. 3*E*,*F*). For these data, a local baseline was established before each action sequence initiation (2 s average, 10 s before the distal press): Preevent background-subtracted signals at the control electrode were subtracted from similarly background-subtracted signals at the glutamate oxidase-coated biosensor to reveal the rapid glutamate concentration changes time-locked to distal and proximal action performance. On average, the largest glutamate transient peak occurred 2.4 s (SEM, 0.2) before the distal action and 2.5 s (SEM, 0.3) before the proximal action. The largest glutamate transient peak before the press was on average 6.8 μM (SEM, 2.2) in amplitude before the distal press and 6.6 μM (SEM, 1.7) before the proximal press. Despite time averaging due to variable transient peak times, these data clearly show that transient glutamate concentration changes occurred when rats were engaged in lever pressing. Statistical analysis of these changes revealed a main effect of time bin (baseline, predistal, or preproximal; $F_{(1,3)} = 7.91$; $p = 0.006$), with *post hoc*

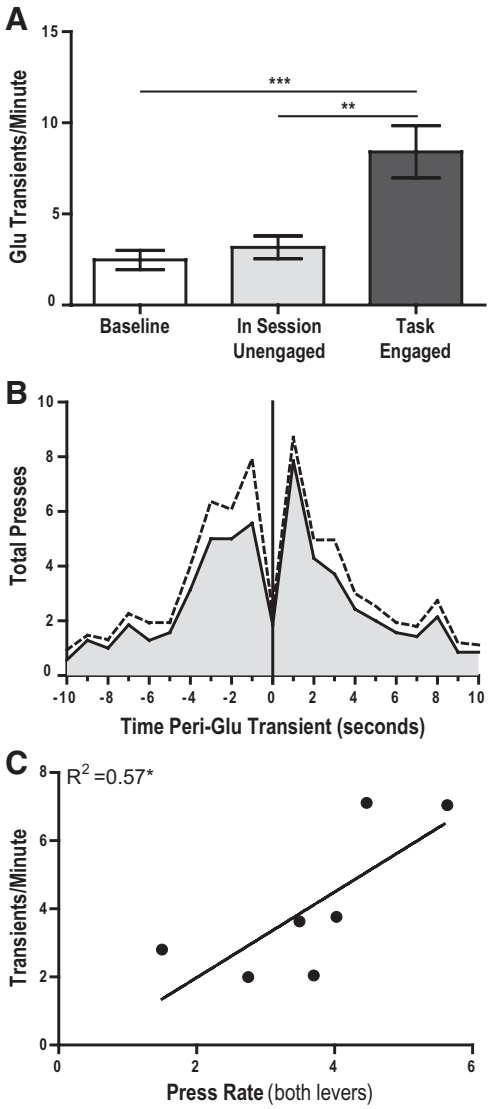

Figure 5. Basolateral amygdala glutamate transient frequency is increased during lever-pressing activity. ***A***, BLA glutamate transient events that reached threshold were counted for the entire test session and then averaged for each rat across the 3 min pre-lever-pressing test baseline period (baseline), during the lever-pressing session when rats were unengaged in the task (in session unengaged), and when rats were engaged in lever pressing (task-engaged). This was then averaged across rats to show that glutamate transient frequency (glutamate transients/minute) was increased when rats were engaged in lever pressing. ***B***, The total number of lever presses (combining both distal and proximal presses) in the 10 s before and after all glutamate transient events were summed for each rat and grouped into 1 s bins (*x*-axis), and then averaged across rats to result in a peri-transient lever press histogram. The dashed line indicates +1 SEM. ***C***, BLA glutamate transient frequency was averaged across the lever-pressing session for each rat (including both the unengaged and task-engaged phases), and this was correlated with each rat's average lever press rate (on both levers). $N = 7$. Error bars indicate ±1 SEM. $^{*}p < 0.05$; $^{**}p < 0.01$; $^{***}p < 0.001$.

analyses confirming that the glutamate concentration peak before both the distal ($p < 0.01$) and proximal ($p < 0.05$) actions were significantly elevated above baseline levels. This finding, that glutamate concentration transients tended to precede lever presses, is notable for a self-paced task, in which performance, of the distal action especially, was not triggered by an experimenter-delivered cue or signal, and suggests that these transients may have occurred during the decision-making process before initiation of the action sequence. Importantly, however, that the transient glutamate elevations also preceded performance of the proximal action (the terminal link in the sequence) suggests that transient glutamate activity is not solely related to the initiating decision.

Table 2. BLA glutamate transient frequency versus behavioral output correlations

	Behavioral output	
Transient feature	Press rate	Sequence time
Whole session		
Frequency		
R (Pearson)	0.368	−0.142
Significance	$p = 0.417$	$p = 0.761$
Amplitude		
R (Pearson)	0.257	−0.215
Significance	$p = 0.578$	$p = 0.644$
Reacquisition period (cycles 1–5)		
Frequency		
R (Pearson)	0.553	−0.318
Significance	$p = 0.198$	$p = 0.487$
Amplitude		
R (Pearson)	−0.019	0.219
Significance	$p = 0.967$	$p = 0.637$
Performance period (cycles 6–30)		
Frequency		
R (Pearson)	0.753*	−0.236
Significance	$p = 0.050$	$p = 0.611$
Amplitude		
R (Pearson)	0.924**	−0.472
Significance	$p = 0.003$	$p = 0.285$

BLA glutamate transient frequency and amplitude during the behavioral test session [divided into the performance (cycles 6–30) and refamiliarization (cycles 1–5) phases] were correlated against combined lever press rate and the average time it took rats to complete each action sequence (from the first initiating distal press to next initiating distal press).

$^{*}p < 0.05$; $^{**}p < 0.01$.

In support of this, not only did glutamate transient frequency increase with lever-pressing activity, these factors were positively correlated across rats during the performance period of the test (i.e., after the initial five "refamiliarization" response–reward cycles: see Table 2 for additional analysis), such that rats displaying high overall glutamate transient frequency (during the entire lever-pressing test both engaged and unengaged phases) performed at higher levels of lever pressing (Fig. 5*C*; $R^2 = 0.57$; $p = 0.05$). Glutamate transient frequency was not correlated with other measurable reward-related behavioral outputs, such as the average time it took rats to complete the action sequence (Table 2).

Basolateral amygdala glutamate transient amplitude tracks instrumental performance

Although the amplitude of the glutamate transients was not significantly higher when rats were engaged in the lever-pressing task relative to unengaged or baseline phases (Fig. 6*A*; $F_{(2,20)} = 1.89$; $p = 0.19$), overall BLA glutamate transient amplitude during the performance phase of the test (both engaged and unengaged phases) was significantly positively correlated with lever-pressing activity during that phase ($R^2 = 0.85$; $p = 0.003$; Fig. 6*B*). Glutamate transient amplitude was not correlated with other measurable behavioral outputs, such as the average time it took rats to complete the action sequence (Table 2). That the amplitude of glutamate transients, which often preceded lever press actions (Fig. 5*B*), predicted the rate with which those actions were performed is supportive of the hypothesis that BLA glutamate transients are related to the decision-making and initiating processes that occur before lever press actions.

Task-related basolateral amygdala glutamate transients are attenuated after reward devaluation

To further test the hypothesis that transient glutamate signaling in the BLA is a correlate of instrumental action performance and decision making, in a second set of rats we experimentally manip-

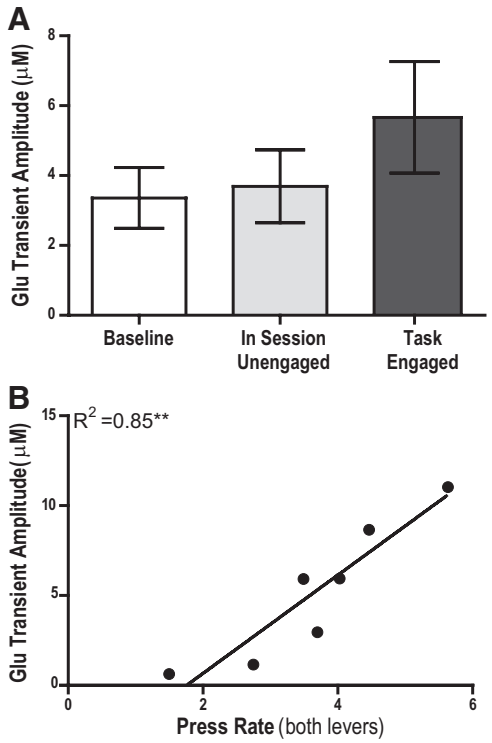

Figure 6. Basolateral amygdala glutamate transient amplitude is associated with lever-pressing activity. ***A***, The amplitude (micromolar) of each glutamate transient event was averaged across the 3 min pre-lever-pressing test baseline period (baseline), during the lever-pressing session when rats were unengaged in the task (in session unengaged), and when rats were engaged in lever pressing (task-engaged). This was then averaged across rats. ***B***, BLA glutamate transient amplitude was average across the lever-pressing session for each rat (including both the unengaged and task-engaged phases), and this was correlated with each rat's average lever press rate (on both levers). $N = 7$. Error bars indicate ± 1 SEM. $^{**}p < 0.01$.

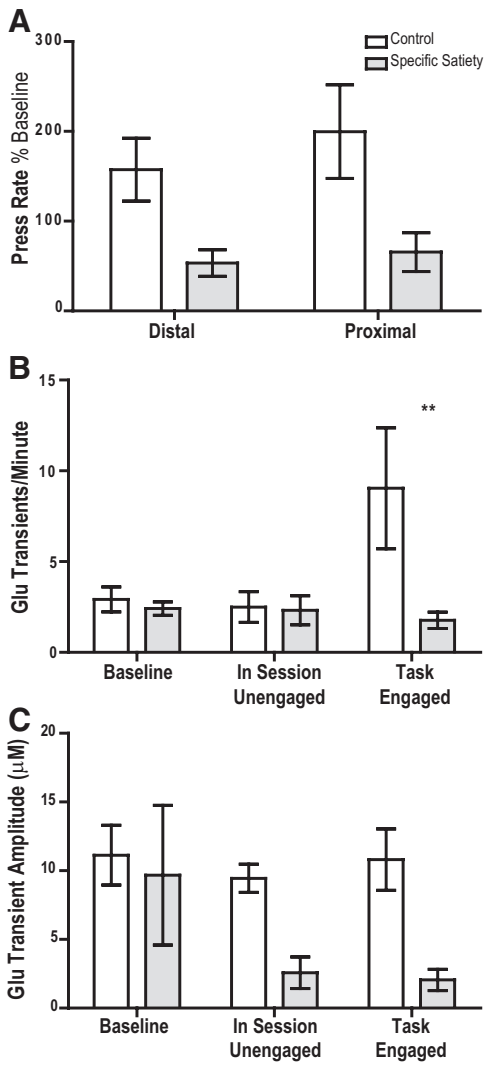

Figure 7. Specific satiety reward devaluation results in a reduction in lever-pressing rate and a concomitant reduction in task-related basolateral amygdala glutamate transient frequency and overall glutamate transient amplitude. ***A***, Effect of specific satiety outcome devaluation on lever-pressing activity. Rats receiving the specific satiety treatment (shaded bars) showed lower distal and proximal response rates (normalized to presatiety baseline levels) than unsated controls (open bars). ***B***, Average BLA glutamate (glu) transient frequency before the behavioral session (baseline) and during the session, separated into unengaged and task-engaged phases. Glutamate transient frequency is increased when rats are engaged in the lever-pressing task, and this effect is blocked in rats receiving the specific satiety devaluation treatment. ***C***, Effect of specific satiety on the average glutamate transient amplitude (micromolar). $N = 4$ per group. Error bars indicate ± 1 SEM. $^{**}p < 0.01$.

ulated the value of the sucrose reward, information that is used to inform decisions, with a specific satiety reward devaluation procedure. We assessed the effects of this manipulation on both lever-pressing activity and transient BLA glutamate concentration changes. After an initial 10 cycle refamiliarization session following sensor implantation and recovery, rats, while in the holding chamber, were either allowed to consume the sucrose pellets to satiety, or given no satiety treatment immediately before being returned to the testing chamber. Such satiety treatment is well established to produce both general motivational-induced and sensory-specific reward value-based reductions in lever pressing (Berridge, 1991; Dickinson et al., 1996; Balleine et al., 2005; Wassum et al., 2009b), an effect that requires an intact BLA (Balleine et al., 2003). Accordingly, rats that received the specific satiety treatment showed significantly lower rates of responding on both levers (main effect of satiety: $F_{(1,6)} = 6.68$, $p = 0.04$; no effect of lever: $F_{(1,6)} = 3.81$, $p = 0.09$; or interaction: $F_{(1,6)} = 1.17$, $p = 0.32$; Fig. 7*A*).

Interestingly, the reduction in lever-pressing activity brought about by specific satiety was accompanied by a decrease in glutamate transient frequency, an effect that was specific to task-related glutamate transients (Fig. 7*B*). Statistical analysis of these data reveals marginally insignificant overall main effects of satiety ($F_{(1,12)} = 1.25$; $p = 0.09$) and test phase (before the session, in the session–outside the 20 s peri-press window, or in the session–task-engaged; $F_{(2,12)} = 2.70$; $p = 0.11$) on glutamate transient frequency. Importantly, there was a significant interaction between these two factors ($F_{(2,12)} = 3.92$; $p = 0.04$). *Post hoc* analyses clarify this interaction to show that glutamate transient frequency was significantly lower in rats that received the specific satiety treatment relative to unsated controls only when the rats were engaged in the task ($p < 0.05$). Indeed, after the specific satiety treatment, rats showed a significantly lower (0.17; SEM, 0.05) transient/press ratio than unsated controls (0.60; SEM, 0.1; $t_{(6)} = 2.45$; $p = 0.05$).

In addition, the amplitude of such transients was also attenuated. Analysis of the data shown in Figure 7*C* reveals a main effect of satiety on average glutamate transient amplitude ($F_{(1,12)} = 6.56$; $p = 0.04$) with no effect of test phase ($F_{(2,12)} = 1.98$; $p = 0.18$), or interaction between these factors ($F_{(2,12)} = 1.21$; $p = 0.33$), suggesting that, unlike the effect on glutamate transient frequency, specific satiety reduced the amplitude of all transient glutamate concentration changes. Thus, BLA glutamate transients related to instrumental activity varied in

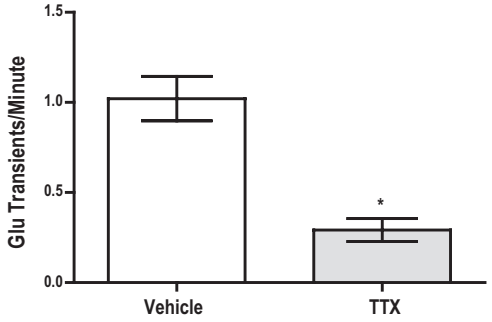

Figure 8. TTX attenuates baseline BLA glutamate transient frequency. TTX (shaded bars) infused locally into the region around the MEA sensor attenuated the frequency of glutamate transients in freely moving rats relative to vehicle infusion (open bars). Rats were not engaged in a lever-pressing task. $N = 4$. Error bars indicate ± 1 SEM. $^{*}p < 0.05$.

frequency and amplitude with changes in lever-pressing activity induced by a reduction in motivational state.

Transient basolateral amygdala glutamate concentration changes are the result of neuronal release

As glutamate can arise from release from both neurons and non-neuronal (i.e., glial) sources, it was imperative to assess the pool from which our glutamate concentration changes arose. Using glutamate biosensors similar to those used in our work, others have shown glutamate concentration changes to be, at least in part synaptic in origin (Belay et al., 1999; Day et al., 2006; Rutherford et al., 2007; van der Zeyden et al., 2008; Hascup et al., 2010). We suspected that the transient glutamate concentration changes we detect in the BLA were similarly the result of neuronal activity. To test this hypothesis, we locally infused TTX (0.3 μl of 100 μM) into the region surrounding the glutamate biosensor to block action potential-dependent glutamate release. In preliminary experiments, this completely blocked lever-pressing performance; we therefore focused on baseline, spontaneous glutamate transient activity in freely moving rats not engaged in lever pressing. The frequency of spontaneous glutamate transients was significantly reduced by TTX (Fig. 8; $t_{(4)} = 4.23$; $p = 0.02$), suggesting that they are likely the result of neuronal release.

Task-related basolateral amygdala glutamate transients are abolished following orbitofrontal cortex inactivation

To further examine the origin of the glutamate transients, we next considered the possible glutamatergic neuronal inputs to the BLA that might contribute to these signals. There are known glutamatergic projections to the BLA from the hippocampus, thalamus, and cortex. Of the cortical inputs, those from the orbital frontal region are particularly strong and reciprocal in nature. Indeed, an interaction between the OFC and BLA has been suggested necessary for goal-directed behavior (Pickens et al., 2003; Schoenbaum et al., 2003; Holland and Gallagher, 2004). Therefore, in a separate set of rats, we inactivated the OFC with ipsilateral infusions of muscimol (0.5 μl of 1 μg/μl) while monitoring transient glutamate concentration changes in the BLA of rats performing on the sequence of actions to earn sucrose pellet rewards. Infusion of muscimol to inactivate the OFC did not impact rats' lever-pressing activity (Fig. 9*A*), most likely because unilateral infusions were intentionally used; statistical analysis showed neither a main effect of drug ($F_{(1,3)} = 1.14$; $p = 0.36$) nor an interaction between the effects of drug and lever ($F_{(1,3)} = 0.29$; $p = 0.62$) on lever press rates. Importantly, between the two vehicle tests, there was no overall main effect of test on either lever press rates

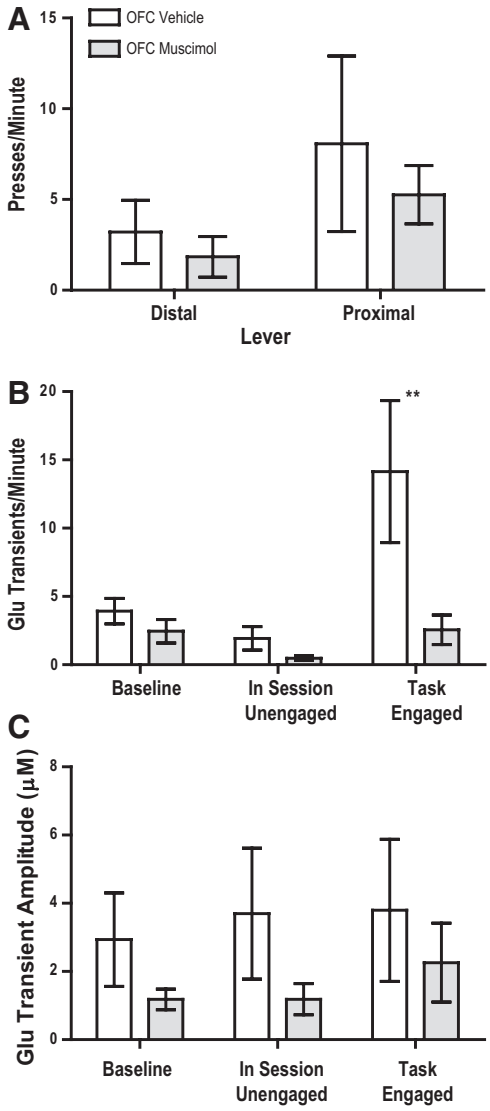

Figure 9. Orbitofrontal cortex inactivation attenuates basolateral amygdala glutamate transients. ***A***, Ipsilateral intra-OFC muscimol infusion (shaded bars) did not impact press rate on either the distal or proximal lever. ***B***, Infusion of muscimol into the OFC decreased the frequency of glutamate (glu) transients when rats were engaged in the behavioral task relative to vehicle infusion (open bars), but did not significantly alter glutamate transient frequency before the behavioral session or when rats were unengaged in lever pressing. ***C***, Glutamate transient amplitude (micromolar) was not significantly affected by intra-OFC muscimol infusion. $N = 4$. Error bars indicate ± 1 SEM. $^{**}p < 0.01$.

($F_{(1,3)} = 0.39$; $p = 0.58$) or glutamate transient frequency ($F_{(2,6)} = 1.35$; $p = 0.33$); therefore, these tests were collapsed for all further analyses.

As is clear from Figure 9*B*, OFC inactivation did, however, significantly attenuate glutamate transients, but only when rats were engaged in the lever press sequence. Statistical analysis of these data reveals a marginal effect of drug ($F_{(1,6)} = 7.52$; $p = 0.07$) and test phase ($F_{(2,6)} = 4.45$; $p = 0.07$), but most importantly a drug by test phase interaction ($F_{(2,6)} = 6.05$; $p = 0.03$). *Post hoc* analyses clarify this interaction to suggest that OFC muscimol infusions decreased glutamate transient frequency only when rats were engaged in the lever press sequence ($p < 0.01$). Indeed, muscimol infusion completely blocked ($F_{(2,6)} = 2.60$; $p = 0.15$) the increase in transient frequency observed in the vehicle-treated condition when rats were engaged in the lever press

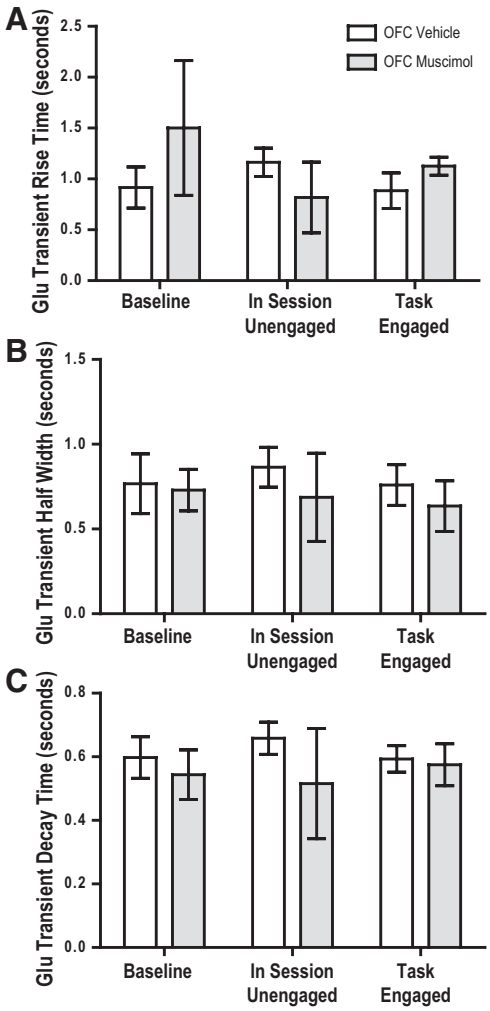

Figure 10. Dynamics of basolateral amygdala glutamate transients are unaltered by orbitofrontal cortex inactivation. ***A***, Glutamate (Glu) transient rise time (seconds) was not affected by either test phase or intra-OFC drug. ***B***, Glutamate transient half-width (seconds) was also not affected by either test phase or intra-OFC drug. ***C***, Glutamate transient decay time (seconds) was unaffected by either test phase or intra-OFC drug. $N = 4$. Error bars indicate ± 1 SEM.

sequence, relative to the baseline period ($F_{(2,6)} = 5.11$; $p = 0.05$). These data indicate that glutamate transients in the BLA that were related to the performance of instrumental actions likely arose from release from neurons with their cell bodies in the OFC.

While OFC inactivation altered BLA glutamate transient frequency, it did not affect the properties of the glutamate transients that did reach threshold, including glutamate transient amplitude; there was no overall main effect of drug on glutamate transient amplitude ($F_{(1,6)} = 1.03$; $p = 0.39$), no effect of session phase ($F_{(2,6)} = 1.98$; $p = 0.22$), and no interaction between these factors ($F_{(2,6)} = 0.53$; $p = 0.54$; Fig. 9*C*). As can be seen in Figure 10, the temporal dynamics of glutamate transients were also unaffected by OFC inactivation. Analysis of glutamate transient rise time revealed no main effect drug ($F_{(1,3)} = 0.55$; $p = 0.51$), test phase ($F_{(2,2)} = 0.13$; $p = 0.89$), or interaction between these variables ($F_{(2,2)} = 0.79$; $p = 0.56$). Similarly, there was no main effect of drug ($F_{(1,3)} = 2.02$; $p = 0.25$), test phase ($F_{(2,2)} = 0.88$; $p = 0.53$), or interaction between these variables ($F_{(2,2)} = 0.13$; $p = 0.90$) on BLA glutamate transient half-width. Last, no effect of drug ($F_{(1,3)} = 0.70$; $p = 0.47$), test phase ($F_{(2,2)} = 0.90$; $p = 0.53$), or interaction between these variables ($F_{(2,2)} = 0.69$; $p = 0.59$) was identified for glutamate transient decay time.

Discussion

Glutamate biosensors were used to identify rapid transient extracellular glutamate fluctuations in the BLA during performance of an instrumental task. The frequency of spontaneous glutamate transients in the BLA increased when rats were engaged in a self-paced lever press sequence to earn sucrose rewards and decreased when the value of the earned reward was reduced by satiety. Glutamate transients tended to precede lever press actions and lever press rate was positively correlated with both transient frequency and amplitude. Lastly, these glutamate transients were action potential dependent and appeared to originate from projections of neurons located in the OFC.

Neuronal origin of glutamate concentration transients in the basolateral amygdala

Escape of glutamate from the synapse is tightly regulated by reuptake transporters predominantly located on glia (Bergles et al., 1999). Indeed, the insensitivity of microdialysis extracellular glutamate measures to TTX and to calcium removal (Miele et al., 1996; Timmerman and Westerink, 1997) indicates that much of the tonic extracellular glutamate originates from nonvesicular release, such as via cysteine/glutamate exchange (Baker et al., 2002). However, reports describing electroenzymatic biosensor measures of tonic glutamate have demonstrated at least a degree of TTX and calcium sensitivity (Belay et al., 1999; Day et al., 2006; Rutherford et al., 2007; van der Zeyden et al., 2008) and have shown that tail pinch stressor-induced increases in glutamate concentration are completely abolished by TTX (Hascup et al., 2010). Importantly, the rapid BLA glutamate transients we observed here were significantly attenuated by TTX and by inhibition of a major cortical glutamatergic input to this region. Together, these data point to a vesicular origin and corroborate electrophysiological evidence of synaptic overspill of glutamate (Bergles et al., 1999; Diamond, 2002).

In the context of extracellular neurochemical recordings, these are quite rapid events, with durations of the order of 2–5 s, comparable with transient dopamine events recorded in the striatum with fast-scan cyclic voltammetry (Wightman et al., 2007) and found to be associated with reward-related behavior (Phillips et al., 2003; Wanat et al., 2009). However, the kinetics of the BLA glutamate transients we observed must be considered in light of the response characteristics of the biosensors. Unlike detection of dopamine, which is essentially limited by diffusion through the extracellular milieu and active reuptake, glutamate detection is additionally impacted by enzyme kinetics and the multiple polymeric layers on the electrode surface. As previously reported (Wassum et al., 2008), the response time of our sensors is ~0.8 s *in vitro*. The transients we observe *in vivo* occur over a comparable time frame and are therefore potentially faster in reality, being time-averaged by the response characteristics of the sensor. In this context, it is notable that the transient events we describe here are considerably faster than the spontaneous baseline fluctuations (~13–18 s duration) in extracellular glutamate recently recorded in the prefrontal cortex using similar sensors, which were not correlated with any behavioral event (Hascup et al., 2011).

The amplitude of the events recorded here, estimated on the basis of *in vitro* calibration data to be in the 1–20 μM range, is sufficient to activate extrasynaptic group 2 metabotropic glutamate receptors, which are considered to mediate presyn-

aptic inhibition following synaptic overflow and thereby provide a negative-feedback mechanism (Scanziani et al., 1997). These concentrations are also adequate to activate synaptic NMDA receptors and may therefore reflect volume glutamate transmission, recently proposed on the basis of electrophysiological and fluorescent reporter measurements (Szapiro and Barbour, 2007; Hires et al., 2008). Moreover, these concentration estimates may be conservative, given that *in vitro* calibration does not take into consideration the potential impact of the extracellular volume fraction and tortuosity *in vivo* (Nicholson and Syková, 1998).

Glutamate transients in the basolateral amygdala track reward-seeking actions

Whether these BLA transients reflect time-averaged "spillout" of synaptic transmission, "spillover" volume transmission, or a combination of the two, their relationship to instrumental behavior, and potentially to the decision-making process itself, is supported by our observations. Not only did the frequency of transients increase during performance of the task, but both the frequency and amplitude of glutamate transients, which often preceded lever presses, positively correlated with response rate. Neither BLA glutamate transient frequency nor amplitude correlated with other measurable behavioral outputs, such as the average time it took rats to complete the action sequence; thus, glutamate transients did not simply track general reward-related behavioral output or motor activity. Moreover, that these correlations were only apparent after the refamiliarization phase (i.e., after an opportunity to be "reminded" of the action–outcome association and therefore be able to use goal value to determine their response rate) suggests that BLA glutamate transient frequency was specifically related to reward-seeking action performance rather than to the general motor activation necessary for lever pressing. That glutamate transients occurred before both the distal and proximal actions in the sequence suggests that they may not be uniquely involved in the decision to initiate the action sequence. Future experiments will explore whether transients associated with the two levers are regulated by different behavioral processes (i.e., incentive value, pavlovian cues, etc.).

The above considerations notwithstanding, the fact that glutamate transients fluctuated with motivational state, and therefore reward value, and tended to precede lever presses (including those that were self-initiated) supports the notion that these signals were related to the decision-making process that guides instrumental action performance. Indeed, the BLA has previously been implicated in goal-directed behavior and reward-related decision making (Balleine et al., 2003; Wellman et al., 2005; Coutureau et al., 2009; Jenison et al., 2011). Our finding that those glutamate concentration transients in the BLA that were specifically related to instrumental actions were diminished by unilateral OFC inactivation may be considered to support a series of reports suggesting that an interaction between the OFC and the BLA is necessary for establishing the value of a reward, and for use of this value to update action performance (Schoenbaum et al., 1998, 2003; Holland and Gallagher, 2004). However, it has also been suggested that, rather than being important for establishing and using incentive value to guide goal-directed actions, the OFC is necessary for the capacity of reward-paired cues, and presumably contexts, to provide predictive information about potential rewarding outcomes (Ostlund and Balleine, 2007a,b). Indeed, many of the aforementioned studies suggesting a role for OFC–BLA interactions in establishing reward value could in fact be reinterpreted as evidence for a role of OFC–BLA interactions in stimulus–outcome learning (Ostlund and Balleine, 2007a,b). Although the two-lever sequence task used in these experiments does not involve explicitly presented reward-paired cues, its performance is undoubtedly guided in part by subtle contextual cues and discriminative stimuli (i.e., insertion of the proximal lever) and likely also by internal signals within the animal. It is therefore alternatively possible, if not likely, that transient glutamate events in the BLA were related to these cues and their ability to facilitate the decision to engage the action sequence and that OFC inactivation reduced these predictive signals. These alternative possibilities are being specifically tested in ongoing experiments.

Those BLA glutamate transients that were not locked to lever-pressing activity may have arisen from a number of other known glutamatergic BLA afferents, including the thalamus, hippocampus, and other cortical regions, or could be the result of release from intrinsic neurons. Future examination of the interplay between these BLA inputs may reveal a more complex circuitry underlying BLA-dependent behaviors, including instrumental behavior.

In summary, an investigation coupling a novel biosensor technology to a self-paced instrumental task revealed rapid transient fluctuations in extracellular glutamate in the BLA that were time-locked to the performance of actions instrumental to gaining rewards, the frequency and amplitude of which were correlated with response rate. Future study of the neuropharmacological modulation of these signals may elucidate the complex BLA neurochemical interactions that underlie reward seeking. Moreover, given the recent suggestion that altered glutamate homeostasis may be critical for long-term drug-seeking behavior (Reissner and Kalivas, 2010), changes in transient BLA glutamate signals arising from administration of abused substances may shed further light on the mechanisms of addiction. More broadly, the ability to monitor discrete behaviorally induced glutamate concentration transients promises to facilitate elucidation of the role of this neurotransmitter in numerous other brain functions and disorders.

References

Baker DA, Xi ZX, Shen H, Swanson CJ, Kalivas PW (2002) The origin and neuronal function of *in vivo* nonsynaptic glutamate. J Neurosci 22:9134–9141.

Balleine BW, Dickinson A (2000) The effect of lesions of the insular cortex on instrumental conditioning: evidence for a role in incentive memory. J Neurosci 20:8954–8964.

Balleine BW, Killcross AS, Dickinson A (2003) The effect of lesions of the basolateral amygdala on instrumental conditioning. J Neurosci 23:666–675.

Balleine B, Paredes-Olay C, Dickinson A (2005) Effects of outcome devaluation on the performance of a heterogeneous instrumental chain. Int J Comp Psychol 18:257–272.

Belay A, Collins A, Ruzgas T, Kissinger PT, Gorton L, Csöregi E (1999) Redox hydrogel based bienzyme electrode for L-glutamate monitoring. J Pharm Biomed Anal 19:93–105.

Bergles DE, Diamond JS, Jahr CE (1999) Clearance of glutamate inside the synapse and beyond. Curr Opin Neurobiol 9:293–298.

Berridge KC (1991) Modulation of taste affect by hunger, caloric satiety, and sensory-specific satiety in the rat. Appetite 16:103–120.

Carmichael ST, Price JL (1995) Limbic connections of the orbital and medial prefrontal cortex in macaque monkeys. J Comp Neurol 363:615–641.

Corbit LH, Muir JL, Balleine BW (2003) Lesions of mediodorsal thalamus and anterior thalamic nuclei produce dissociable effects on instrumental conditioning in rats. Eur J Neurosci 18:1286–1294.

Coutureau E, Marchand AR, Di Scala G (2009) Goal-directed responding is sensitive to lesions to the prelimbic cortex or basolateral nucleus

of the amygdala but not to their disconnection. Behav Neurosci 123:443–448.
Day BK, Pomerleau F, Burmeister JJ, Huettl P, Gerhardt GA (2006) Microelectrode array studies of basal and potassium-evoked release of L-glutamate in the anesthetized rat brain. J Neurochem 96:1626–1635.
Diamond JS (2002) A broad view of glutamate spillover. Nat Neurosci 5:291–292.
Dickinson A, Campos J, Varga ZI, Balleine B (1996) Bidirectional instrumental conditioning. Q J Exp Psychol B 49:289–306.
Ghashghaei HT, Barbas H (2002) Pathways for emotion: interactions of prefrontal and anterior temporal pathways in the amygdala of the rhesus monkey. Neuroscience 115:1261–1279.
Hamdi NWJ, Walker E, Maidment NT, Monbouquette HG (2006) An electroenzymatic L-glutamate microbiosensor selective against dopamine. J Electroanal Chem 591:33–40.
Hascup ER, Hascup KN, Stephens M, Pomerleau F, Huettl P, Gratton A, Gerhardt GA (2010) Rapid microelectrode measurements and the origin and regulation of extracellular glutamate in rat prefrontal cortex. J Neurochem 115:1608–1620.
Hascup KN, Hascup ER, Stephens ML, Glaser PE, Yoshitake T, Mathé AA, Gerhardt GA, Kehr J (2011) Resting glutamate levels and rapid glutamate transients in the prefrontal cortex of the flinders sensitive line rat: a genetic rodent model of depression. Neuropsychopharmacology 36:1769–1777.
Hires SA, Zhu Y, Tsien RY (2008) Optical measurement of synaptic glutamate spillover and reuptake by linker optimized glutamate-sensitive fluorescent reporters. Proc Natl Acad Sci U S A 105:4411–4416.
Holland PC, Gallagher M (2004) Amygdala-frontal interactions and reward expectancy. Curr Opin Neurobiol 14:148–155.
Hu Y, Mitchell KM, Albahadily FN, Michaelis EK, Wilson GS (1994) Direct measurement of glutamate release in the brain using a dual enzyme-based electrochemical sensor. Brain Res 659:117–125.
Jenison RL, Rangel A, Oya H, Kawasaki H, Howard MA (2011) Value encoding in single neurons in the human amygdala during decision making. J Neurosci 31:331–338.
Johnson AW, Bannerman DM, Rawlins NP, Sprengel R, Good MA (2005) Impaired outcome-specific devaluation of instrumental responding in mice with a targeted deletion of the AMPA receptor glutamate receptor 1 subunit. J Neurosci 25:2359–2365.
Johnson AW, Bannerman D, Rawlins N, Sprengel R, Good MA (2007) Targeted deletion of the GluR-1 AMPA receptor in mice dissociates general and outcome-specific influences of appetitive rewards on learning. Behav Neurosci 121:1192–1202.
Kelley AE (2004) Ventral striatal control of appetitive motivation: role in ingestive behavior and reward-related learning. Neurosci Biobehav Rev 27:765–776.
Kulagina NV, Shankar L, Michael AC (1999) Monitoring glutamate and ascorbate in the extracellular space of brain tissue with electrochemical microsensors. Anal Chem 71:5093–5100.
Lowry JP, Ryan MR, O'Neill RD (1998) Behaviourally induced changes in extracellular levels of brain glutamate monitored at 1 s resolution with an implanted biosensor. Anal Commun 35:87–89.
Mar AC, Walker AL, Theobald DE, Eagle DM, Robbins TW (2011) Dissociable effects of lesions to orbitofrontal cortex subregions on impulsive choice in the rat. J Neurosci 31:6398–6404.
Michael DJ, Joseph JD, Kilpatrick MR, Travis ER, Wightman RM (1999) Improving data acquisition for fast-scan cyclic voltammetry. Anal Chem 71:3941–3947.
Miele M, Boutelle MG, Fillenz M (1996) The source of physiologically stimulated glutamate efflux from the striatum of conscious rats. J Physiol 497:745–751.
Nicholson C, Syková E (1998) Extracellular space structure revealed by diffusion analysis. Trends Neurosci 21:207–215.
Ostlund SB, Balleine BW (2007a) Orbitofrontal cortex mediates outcome encoding in pavlovian but not instrumental conditioning. J Neurosci 27:4819–4825.
Ostlund SB, Balleine BW (2007b) The contribution of orbitofrontal cortex to action selection. Ann N Y Acad Sci 1121:174–192.
Paxinos G, Watson C (1998) The rat brain in stereotaxic coordinates, 4th ed. San Diego: Academic.
Phillips PE, Stuber GD, Heien ML, Wightman RM, Carelli RM (2003) Subsecond dopamine release promotes cocaine seeking. Nature 422:614–618.
Pickens CL, Saddoris MP, Setlow B, Gallagher M, Holland PC, Schoenbaum G (2003) Different roles for orbitofrontal cortex and basolateral amygdala in a reinforcer devaluation task. J Neurosci 23:11078–11084.
Pickens CL, Saddoris MP, Gallagher M, Holland PC (2005) Orbitofrontal lesions impair use of cue-outcome associations in a devaluation task. Behav Neurosci 119:317–322.
Pomerleau F, Day BK, Huettl P, Burmeister JJ, Gerhardt GA (2003) Real time in vivo measures of L-glutamate in the rat central nervous system using ceramic-based multisite microelectrode arrays. Ann N Y Acad Sci 1003:454–457.
Ray JP, Price JL (1992) The organization of the thalamocortical connections of the mediodorsal thalamic nucleus in the rat, related to the ventral forebrain-prefrontal cortex topography. J Comp Neurol 323:167–197.
Reissner KJ, Kalivas PW (2010) Using glutamate homeostasis as a target for treating addictive disorders. Behav Pharmacol 21:514–522.
Rutherford EC, Pomerleau F, Huettl P, Strömberg I, Gerhardt GA (2007) Chronic second-by-second measures of L-glutamate in the central nervous system of freely moving rats. J Neurochem 102:712–722.
Ryan MR, Lowry JP, O'Neill RD (1997) Biosensor for neurotransmitter L-glutamic acid designed for efficient use of L-glutamate oxidase and effective rejection of interference. Analyst 122:1419–1424.
Scanziani M, Salin PA, Vogt KE, Malenka RC, Nicoll RA (1997) Use-dependent increases in glutamate concentration activate presynaptic metabotropic glutamate receptors. Nature 385:630–634.
Schoenbaum G, Chiba AA, Gallagher M (1998) Orbitofrontal cortex and basolateral amygdala encode expected outcomes during learning. Nat Neurosci 1:155–159.
Schoenbaum G, Setlow B, Saddoris MP, Gallagher M (2003) Encoding predicted outcome and acquired value in orbitofrontal cortex during cue sampling depends upon input from basolateral amygdala. Neuron 39:855–867.
Szapiro G, Barbour B (2007) Multiple climbing fibers signal to molecular layer interneurons exclusively via glutamate spillover. Nat Neurosci 10:735–742.
Timmerman W, Westerink BH (1997) Brain microdialysis of GABA and glutamate: what does it signify? Synapse 27:242–261.
van der Zeyden M, Oldenziel WH, Rea K, Cremers TI, Westerink BH (2008) Microdialysis of GABA and glutamate: analysis, interpretation and comparison with microsensors. Pharmacol Biochem Behav 90:135–147.
Wanat MJ, Willuhn I, Clark JJ, Phillips PE (2009) Phasic dopamine release in appetitive behaviors and drug addiction. Curr Drug Abuse Rev 2:195–213.
Wassum KM, Tolosa VM, Wang J, Walker E, Monbouquette HG, Maidment NT (2008) Silicon wafer-based platinum microelectrode array biosensor for near real-time measurement of glutamate in vivo. Sensors 8:5023–5036.
Wassum KM, Ostlund SB, Maidment NT, Balleine BW (2009a) Distinct opioid circuits determine the palatability and the desirability of rewarding events. Proc Natl Acad Sci U S A 106:12512–12517.
Wassum KM, Cely IC, Maidment NT, Balleine BW (2009b) Disruption of endogenous opioid activity during instrumental learning enhances habit acquisition. Neuroscience 163:770–780.
Wellman LL, Gale K, Malkova L (2005) $GABA_A$-mediated inhibition of basolateral amygdala blocks reward devaluation in macaques. J Neurosci 25:4577–4586.
Wightman RM, Heien ML, Wassum KM, Sombers LA, Aragona BJ, Khan AS, Ariansen JL, Cheer JF, Phillips PE, Carelli RM (2007) Dopamine release is heterogeneous within microenvironments of the rat nucleus accumbens. Eur J Neurosci 26:2046–2054.